FACTA UNIVERSITATIS
Series: **Electronics and Energetics** Vol. 33, N° 3, September 2020, pp. 429-444
https://doi.org/10.2298/FUEE2003429T

TECHNIQUE OF CONTROL PMSM POWERED BY PV PANEL USING PREDICTIVE CONTROLLER OF DTC-SVM

Fadila Tahiri, Abdelkader Harrouz, Djamel Belatrache, Fatiha Bekraoui, Ouledali Omar, Ibrahim Boussaid

Department of Hydrocarbon and Renewable Energy, Laboratory LDDI,
University of Ahmed Draya, Adrar, Algeria

Abstract. *The present paper is a part of the study of Direct Torque Control based (DTC) on space vector modulation using predictive controller (Predictive SVM) of a permanent magnet synchronous motor (PMSM) powered by a photovoltaic (PV) source. In the conventional direct torque control (DTC) of a permanent magnet synchronous motor (PMSM), hysteresis controllers are used to choose the proper voltage vector resulting in large torque ripples. The direct torque control can accelerate the torque responses but increases the torque ripple at same time. Nowadays, exist some other alternative approaches to reduce the torque ripples based on (Predictive SVM) technique. This method is based on the replacement of hysteresis comparators (used in conventional DTC) by Proportional Integral (PI) regulators and the selection table by space vector modulation (SVM). The simulation results confirm that this proposed method where the control of the switching frequency is well controlled, allows us to reduce the oscillations of the electromagnetic torque and flux by 20 % and 30%, respectively with a good dynamic response compared with conventional DTC.*

Key words: photovoltaic, PMSM, DTC, DTC-SVM, predictive controller.

NOMENCLATURE

I_0	Reverse saturation current of the diode (A)
I_{0r}	Reverse saturation current
K	Constant of Boltzmann (1.38.10-23J / K)
q	Charge of the electron (1.6.10-19C)
a	p-n junction ideality factor
E_G	Band gap
G, G_r	Real and reference solar radiation
I_{cc}	Short-circuit current
$v_{s\alpha}$, $v_{s\beta}$ $I_{s\alpha}$, $I_{s\beta}$ $\varphi_{s\alpha}$, $\varphi_{s\beta}$	Current, voltage and magnetic flux of stator (α,β)axes

Received December 31, 2019; received in revised form May 17, 2020
Corresponding author: Abdelkader Harrouz
Department of Renewable Energy and Hydrocarbon, Faculty of Technology and Sciences, Ahmed Draïa University - Adrar, Algeria
E-mail: harrouz.onml@gmail.com

ω	The speed of rotation of the machine (rotor)(rad/s)
ϕ_f	Permanent magnet flux linkage (web)
R_s	The stator resistance (Ω)
L_s	The inductance of the stator(H)
J	Moment of inertia
f	Coefficient of friction
P	Number of pairs of poles
$V_{a,b,c}$, $I_{a,b,c}$	Three-phase voltage and current

1. INTRODUCTION

The demand for electrical energy increases daily to cover human needs; the use of renewable energy is becoming the key solution to this serious energy crisis and environmental pollution [1]. Algeria has great potential from solar energy, because it has a vast desert area and very high solar radiation [2-3]. For this reason, the optimal solution to energy production in our study is solar energy [4]. In the field of variable speed, the permanent magnet synchronous machine are extensively accepted due to their high efficiency, high power density, high precision, low maintenance costs, simple structure, and its high torque density [5-6]. Among the most used applications for the permanent magnet synchronous motor (PMSM) are drones, portable robots, and vacuum pumps for decades of diversity and performance. Especially in electric and hybrid cars [7]. Vector controlled PMSM drive provides better dynamic response and lesser torque ripples, and necessitates only a constant switching frequency [8]. PMSM modeling has been tackled in the literature in various ways, commonly using a transition of the electrical component from the physical 3-phase structure to an equivalent 2-phase right-angled structure, enabled by the Clark Transformation [9]. Due to the presence of external disturbances and parameter variation in PMSM over the past decades, performance has been improved by developing various powerful control technologies. [10] However, the widely used approach consists in using linear control theory with the disturbance estimate [11]. It is therefore interesting to find a way to make their independent control to improve their performance. The most suitable solution now is direct torque control (DTC). This method has been first proposed for induction machines [7-12]. It is used in variable frequency drives where the stator flux and machine electromagnetic torque are directly used to generate the control pulses for voltage-source inverter through a predefined switching table [13], DTC owns the advantages of simplicity, quick dynamic response and robustness, which makes it a powerful motor control method in various applications [14]. However, it is known that DTC is troubled by the disadvantages of large torque/flux ripples and unstable switching frequency [15], which hinders its practiitcal applications. In order to tackle the problems associated with conventional DTC, lots of modified DTC methods are proposed to improve the control performance [16]. Abdelkarim Ammar et al [17], are present the space vector modulation (SVM) based Direct Torque Control strategy (DTC) for induction motor (IM) in order to overcome the drawbacks of the classical DTC. Moreover, they proposed model based loss minimization strategy for efficiency optimization, the proposed SVM-DTC algorithm was investigated by using Matlab/ Simulink with real time interface based on dSpace 1104 signal card. The simulation and experimental validation gives similar results, they showed

that LMC reduces losses, improved efficiency at zero and low loads operation. Therefore, DTC-SVM it's a good solution in general to overcome the drawbacks of classical DTC. A comprehensive review has been provided by R H Kumar et al [18] of recent advancements of DTC of induction motor (IM) for the past one decade. Strategies adopted to improve the performance of DTC based on switching table, constant switching frequency operation, intelligent control, sensor less control and predictive control are extensively discussed with its key results and algorithms. The simulation results of DTC Predictive show a reduction in torque and stator flux ripples by 14.94 and 23%, respectively, compared with conventional DTC drive.

In this paper, we use the control Predictive DTC-SVM applied to Permanent Magnet Synchronous Motor, to obtain a constant switching frequency after it was variable in conventional DTC (because of the use of hysteresis comparators) and minimize the ripple of torque and flux. This method of control (Predictive DTC-SVM) is based on the replacement of hysteresis comparators (used in conventional DTC) [17] by Proportional Integral (PI) regulators and the selection table by space vector modulation (SVM).[21]

2. MODELING SYSTEM

2.1. Photovoltaic System

The solar cells are generally connected in series and in parallel, in parallel with Nph cells to increase the current and in series with Nsh cells to increase the voltage then increase the PV power. A PV generator is made up of interconnected modules to form a unit producing high continuous power compatible with conventional electrical equipment [19]. The used model is shown in Figure.1, which consists of four components: a current generator I_{ph}, a diode, a parallel resistance R_{sh} and a serial resistance R_{se} [20].

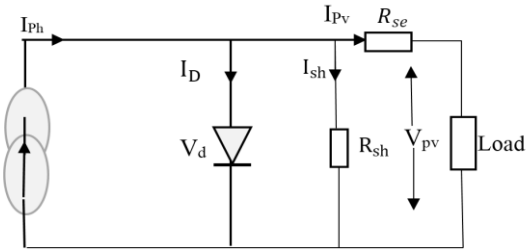

Fig. 1 Equivalent diagram of a photovoltaic cell.

The output current is given by the following equation [22]:

$$I_{PV} = N_{sh} I_{ph} - N_{sh} I_0 \left\{ \exp\left[\frac{q\left(V_{pv} + \frac{N_s}{N_{sh}} I_{pv} R_{se} \right)}{akTn_s} \right] - 1 \right\} - \frac{V_{pv} + \frac{N_s}{N_{sh}} I_{pv} R_{se}}{\frac{N_s}{N_{sh}} R_{sh}} \quad (1)$$

Where, the cell reverse saturation current is related to the temperature (T) as follows

$$I_0 = I_{0r}\left(\frac{T}{T_r}\right)^3 \exp\left\{\frac{qE_G}{ka}\left[\frac{1}{298}-\frac{1}{T}\right]\right\} \tag{2}$$

Similarly, the photocurrent Iph depends on the solar radiation (G) and the cell temperature (T) [21]:

$$I_{ph} = I_{cc}\left(\frac{G}{G_r}\right) \tag{3}$$

2.2. Model of PMSM

Accounting for the hypothesis commonly considered in AC machine modelling, the electrical equations of the PMSM in a (α, β) reference frame, are

$$\begin{cases} v_{s\alpha} = R_s.I_{s\alpha} + L_s\dfrac{dI_{s\alpha}}{dt} - \omega.\phi_f.\sin\theta \\ v_{s\beta} = R_s.I_{s\beta} + L_s\dfrac{dI_{s\beta}}{dt} - \phi_f\omega.\cos\theta \\ J\dfrac{d\omega}{dt} = \phi_f.P.\sin\theta.I_{s\alpha} + \phi_f.P.\cos\theta.I_{s\beta} - f\omega - T_r \\ \dfrac{d\theta}{dt} = \omega \end{cases} \tag{4}$$

The electromagnetic torque T_e is given from [23, 38]:

$$T_e = \frac{3}{2}p(\varphi_{s\alpha}I_{s\beta} - \varphi_{s\beta}I_{S\alpha}) \tag{5}$$

2.2.1. Simulation and interpretation

In the first step, we use a simulation of the (PMSM) operation in the reference frame (α, β) powered directly by 50v, 50Hz network.

The software used in this simulation is MATLAB / SIMULINK. We see in (Figure 2.a) that the space of speed reaches the steady state very quickly with an acceptable response time. After applying the load at the moment (0.3s - 0.4s) we found that the speed decreases and then returns to its reference value. The torque peaks at the first start moment, then reaches his value when the speed decreases (under load) and is proportional to the current. (Figure 2.d) shows the temporal evolution of the stator flux, which has a disturbed sinusoidal shape.

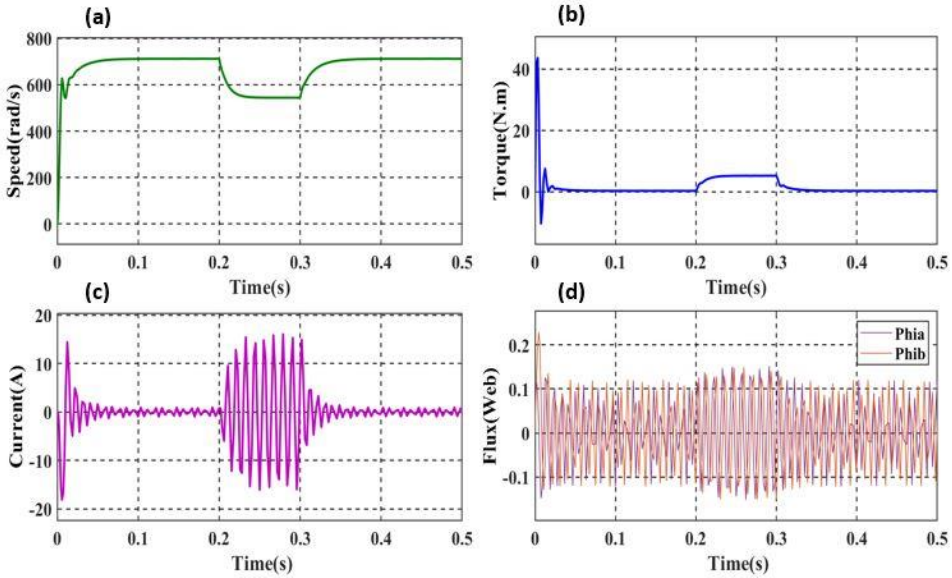

Fig. 2 The variation with time: (a) Speed variation, (b) Torque variation, (c) Current variation, (d) Flux variation.

3. DIRECT TORQUE CONTROL OF PMSM

The block scheme of the investigated direct torque control (DTC) for a voltage source inverter fed PMSM is presented in Figure.3

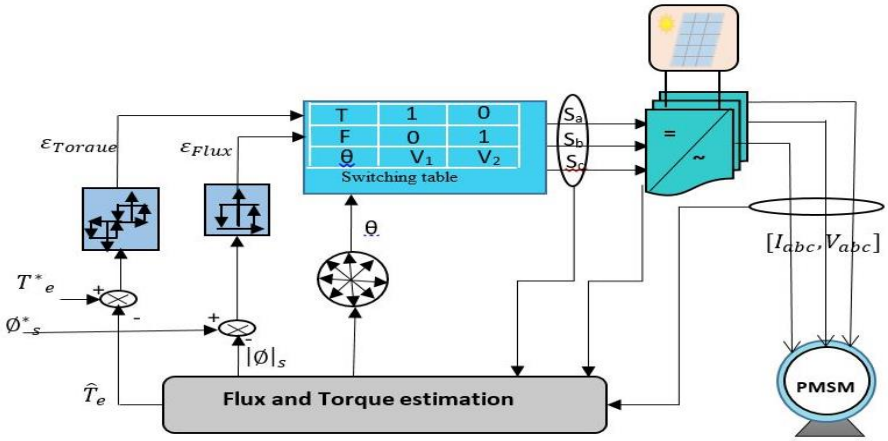

Fig. 3 General structure of the DTC.

The direct torque control of a permanent magnet synchronous machine is based on direct determination of the control sequence to be applied to a voltage inverter [24]. The switching states is selected from the two comparator output (error) of both torque and flux, where the estimated values of torque and flux are compared with the reference values and depending upon the hysteresis comparator error, the result may increase or decreases [25]. The estimation of reference torque, flux and position of flux vector is done by using machine input voltages and currents as shown in Figure.3 [26]

The stator electric equations of the PMSM, in a (α, β) reference frame are given by [27]:

$$\begin{cases} \mathrm{I}_{s\alpha} = \sqrt{\frac{3}{2}}.I_{sa} \\ I_{S\beta} = \frac{1}{\sqrt{2}}(I_{sb} - I_{sc}) \\ \overline{I_s} = \mathrm{I}_{s\alpha} + j.I_{S\beta} \end{cases} \tag{6}$$

The stator voltage:

$$\begin{cases} \mathrm{v}_{s\alpha} = \sqrt{\frac{3}{2}}.\left(V_a - \frac{1}{2}(V_b - V_c)\right) = \sqrt{\frac{3}{2}}.U_{dc}\left(S_a - \frac{1}{2}(S_b - S_c)\right) \\ V_{S\beta} = \frac{1}{\sqrt{2}}(V_b - V_c) = \frac{1}{\sqrt{2}}U_{dc}(S_b - S_c) \\ \overline{V_s} = \mathrm{V}_{s\alpha} + j.V_{S\beta} \end{cases} \tag{7}$$

Two-level inverter is capable of producing six non-zero voltage vectors and two zero vectors. Figure.4. shows the complex plane of the eight voltage vectors [28]

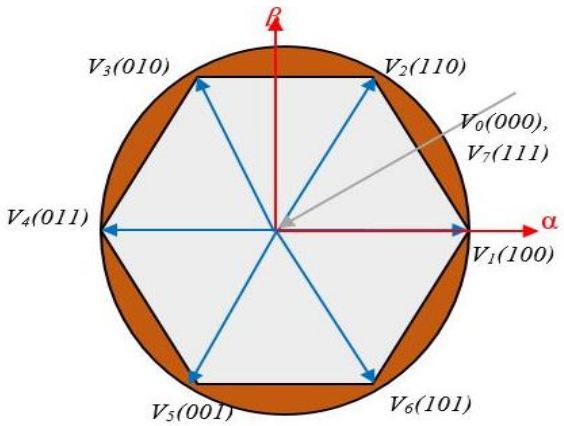

Fig. 4 Different vectors of stator voltages provided by a two levels inverter.

Table 1 shows the switching states to select a suitable V for selecting the switches in the inverter. This voltage sector is generated from the two-comparator output (error) of both torque and flux [25]. The switching table receives 6 active and 2 zero vector from the comparator output and generates 8 possible switching vector for the inverter [27, 29]. DTC select the active voltage switching vector states for doubling the sampling period and select an appropriate V[30].

Table 1 Switching table for DTC 6sector[29].

sector		S1	S_2	S_3	S_4	S_5	S_6
$\Delta_{\varphi s}= 1$	$\Delta T_e = 1$	V_2	V_3	V_4	V_5	V_6	V6
	$\Delta T_e = 0$	V_7	V_0	V_7	V_0	V_7	V_0
	$\Delta T_e = -1$	V_6	V_1	V_2	V_3	V_4	V_5
$\Delta_{\varphi s}= 0$	$\Delta T_e = 1$	V_3	V_4	V_5	V_6	V_1	V_2
	$\Delta T_e = 0$	V_0	V_7	V_0	V_7	V_0	V_7
	$\Delta T_e = -1$	V_5	V_6	V_1	V_2	V_3	V_4

The conventional DTC control is more robust compared against the conventional methods (field-oriented control for example). It does not require a mechanical measurement such as that the speed or position of the machine, moreover the sensitivity to the parameters of the machine is clearly attenuated in the case of DTC, since the flux is made according to a single parameter namely the stator resistance. In addition, SVM (space vector modulation) is replaced in this command by a simple switching table that makes it easier [31].

4. PREDICTIVE DTC-SVM

The strategy of the control DTC-SVM with a predictive controller uses a SVM with a fixed and constant switching frequency [28]. This control strategy ensures the decoupling between the stator flux vectors amplitude and its arguments. Indeed, the stator flux amplitude will be imposed. Nevertheless, the argument is calculated to obtain high performance like the reduction of the stator flux and the electromagnetic torque ripples. The difference between the conventional DTC and this control strategy is that the latter is based on the PI controllers and the SVM in order to fix the switching frequency, which consequently reduces the stator flux and the torque ripples as well as the harmonic waves of the stator current. The switching table and the hysteresis regulators used in the conventional DTC are eliminated. The voltage vector was calculated by using a predictive controller. [29]

The block diagram of the predictive (DTC-SVM) control of a PMSM powered by a voltage inverter from a PV source is shown in Figure 5, the PI Predictive Controller is shown in Figure 6. [32]

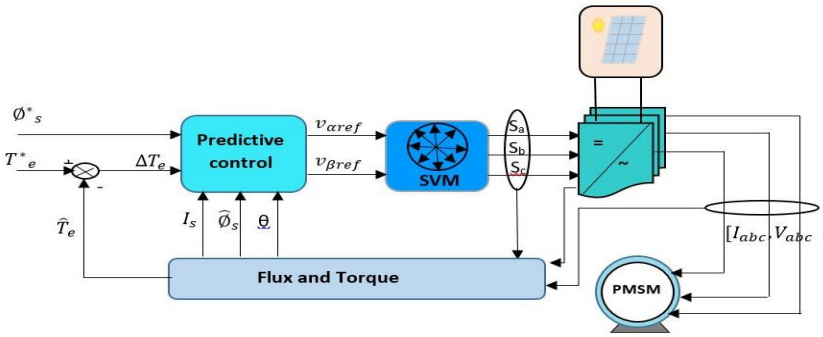

Fig. 5 PMSM system control based on Predictive DTC-SVM.

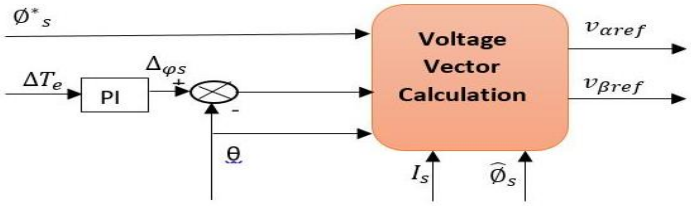

Fig. 6 PI Predictive Controller.

4.1. Predictive Controller

The relationship between the torque pulses: [33]

$$\frac{\Delta T_e}{T_{eref}} = K_s \left| \frac{\Delta \phi_s}{\phi_{sref}} \right| + K_\varphi \Delta\varphi \tag{8}$$

Where T_{eref} the reference is torque, $\Delta\phi_s$ and $\Delta\varphi$ are respectively the deviations from $|\phi_s|$ and φ which are defined by:

$$\begin{aligned} \Delta\phi_s &= |\phi_{sref}| - |\phi_s| \\ \Delta\varphi &= \angle\phi_{sref} - \angle\phi_s \end{aligned} \tag{9}$$

Where K_s and K_φ are the constants derived from the PMSM specifications.

The torque ripple is actually caused by$\Delta\emptyset_s$, $\Delta\varphi$ and the influence of $\Delta\emptyset_s$ is considerably lower than $\Delta\varphi$. As a result, the torque ripple can be attenuated if $\Delta\varphi$ is kept close to zero. For DTC-SVM control, the generation of the control pulses (S_a, S_b, S_c) applied to the inverter switches is generally based on the use of a predictive controller, which receives information about the error of the controller. $\Delta T_e = (T_{e\text{-}ref} - T_e)$ the reference stator flux amplitude $\emptyset_{ref}$, the amplitude and the position of the estimated stator flux vector and the current value to be measured [34]. The predictive controller determines the control reference stator voltage

vector in the polar coordinates V_s= [V_{sref} Δφ]. The equation shows that the relationship between the torque error and the increment of the angle Δφ is linear. Therefore a Proportional Integral (PI) predictive Controller which generates the load angle changing to minimize the instantaneous error between the reference torque and the actual torque, is applied. From the structure of the predictive torque and stator flux controller shown in Figure.6. We noted that the torque error ΔTe and the stator reference flux are delivered to the predictive controller, which gives the deviation of the stator flux angle Δφ [32].

From figure 6; α, β axes components of the stator reference voltage V_{Sref}, are calculated as:

$$\begin{cases} V_{s\alpha ref} = \dfrac{\phi_{sref}\cos(\Delta\varphi+\varphi)-\phi_{sref}\cos\varphi}{T_e} + R_s I_{s\alpha} \\ V_{s\beta ref} = \dfrac{\phi_{sref}\sin(\Delta\varphi+\varphi)-\phi_{sref}\sin\varphi}{T_e} + R_s I_{s\beta} \end{cases} \quad (10)$$

4.2. Space Vector Modulation (SVM)

The SVM method generates the switching signals based on the instantaneous position of the rotating reference vector in the voltage vector space of the converter [14, 37] as shown in the figure.3. In the space vector diagram SVD of a two-level inverter [35], every sector (represented as S_i, i = 1 to 6) is an equilateral symmetrical triangle of height h (=√3/2). The edge vectors (V1 to V6) are named active vectors and (V0, V7) zero vectors. The three closest switching vectors (one zero vector and two active vectors), allows us to calculate the SVM switching time in any sector.

The movement of the reference vector V * positioning inside the sector synthesizing the switching times. Figure 7 allows us to understand the two-level switching of SVD. The determination of the volts-second of V * and their time integral is shown in equation 11. [36]

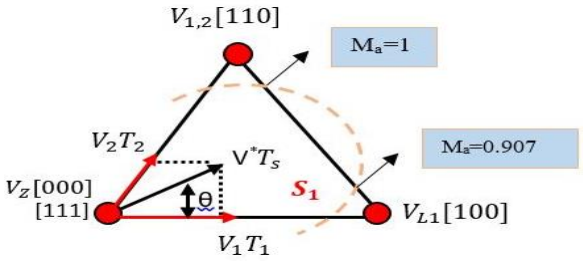

Fig. 7 Sector-1 for two-level SVD

The reference voltage V*volts-sec is calculated by the following equation;

$$V^*T_s = T_1 V_1 + T_2 V_2 + T_0 V_0 \quad (11)$$

Where T_0, T_1 and T_2 are the work times of basic space voltage vector V_0, V_1 and V_2 respectively. V_0 state can be either [000] or [111] switching state, or else both. Equation (12) can be used to determine the position of the angle V * (θ) in the sector;

$$\theta = \text{arctg}\left(\frac{V_{s\alpha}}{V_{s\beta}}\right) \tag{12}$$

The θ values sample the V* in different sector (Example, θ =115°, the V* approach sector-2, since sector-2 lies in an angle between 61°-120°). According to the V* position, whether inside or outside the hexagonal SVD (Figure.7), SVD is divided into linear modulation and over modulation equal Ma ≤0.907and Ma > 0.907, respectively.
$T_S = T_1 + T_2 + T_0$. We calculated T_1 and T_2 from projecting V* position along α-axis and β-axis with respect to SVD origin (zero point). Henceforth, the volts-sec equations for α-axis and β-axis are $V_{S\alpha 0}$ and $V_{S\beta 0}$, $T_S = T_1 + 0.5T_2$ and $T_S = hT_2$, respectively. Thus, $T_2 = T_S V_{S\beta 0}/h$ and $T_1 = T_S (V_{S\alpha 0} - V_{S\beta 0})/2h$. The active vector times T_1 and T_2, help to find the zero voltage time T_S, from the given switching frequency. [37]

5. SIMULATION AND INTERPRETATION

Both the simulations (simulation result of DTC conventional and Predictive DTC-SVM) were proceeded at the same conditions regarding motor parameters, switching frequency of inverter transistors and nominal condition (irradiation, temperature) of PV source. For constant flux operating condition, the flux amplitude produced by permanent magnet is the value of reference amplitude of stator flux. The system consists of photovoltaic sources, inverter, and permanent magnet synchronous motor.

Table 2 Machine and control parameters

Rated motor power	P_n	1.1 kW
Nominal motor voltage	V_n	220V
Power factor	Cos φ	0.38
nominal frequency	f	50Hz
Stator resistance	R_s	0.6 Ohm
Direct stator induction	aL_d	2.8mH
Quadratic stator induction	L_q	1.4mH
Flux of magnets	$\emptyset_f$	0.12Web
Number of pole pairs	P	4
Moment of Inertia	J	$1.1*10^{-3}$ N.m.s^2
Coefficient of friction	f	$1.4*10^{-3}$
nominal torque	T_e	10 N.m

5.1. Simulation Results of Conventional DTC

In Fig.8.b, the electromagnetic torque is illustrated, that begins with a value of approximately 5Nm then its follows the reference torque to return the machine to the previously speed defined by the set point with a reversal of direction of rotation (t = 0.2 to 0.25), finally returns to zero until we apply a load of 5N.m at t= 0.3. We observe in

Fig. 9.a. the stator current temporal evolution, which has an almost sinusoidal shape when we apply a load with an oscillation equal 4 A. The stator flux module follows its reference without exceeding. It shows no sensitivity to the load application. We noted that the electromagnetic torque is full of ripples caused by the used of hysteresis controllers for the stator flux and the electromagnetic torque ,which introduce limitations such as a variable switching frequency, high flux ripples and current distortion.

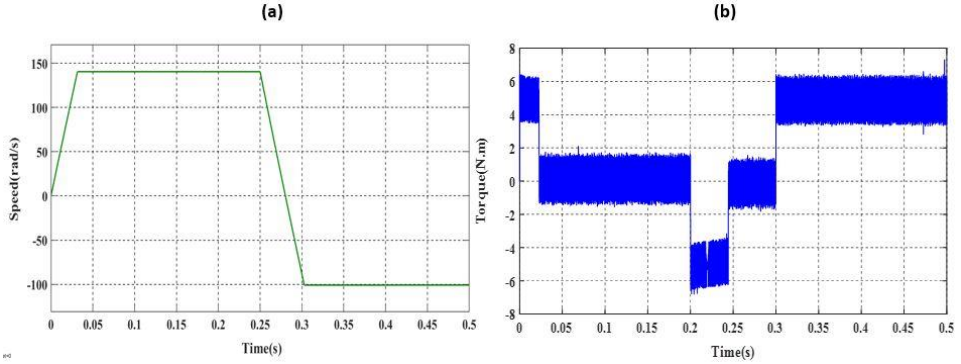

Fig. 8 (a) –The variation of speed responses, (b) –The variation of stator torque responses

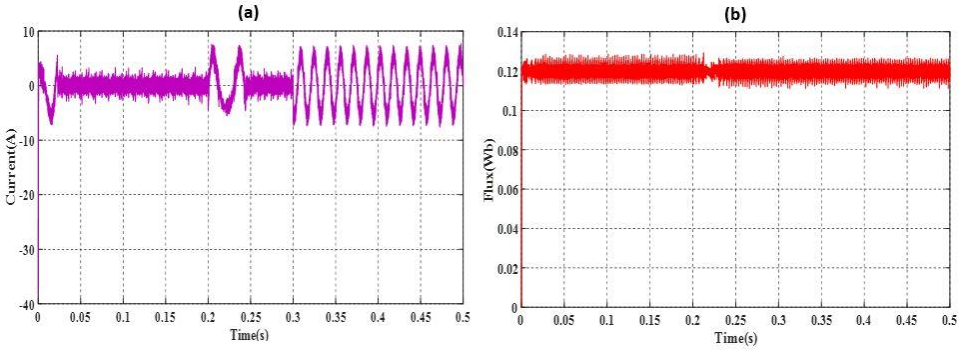

Fig. 9 (a) –The variation of current responses, (b) –The variation of flux responses

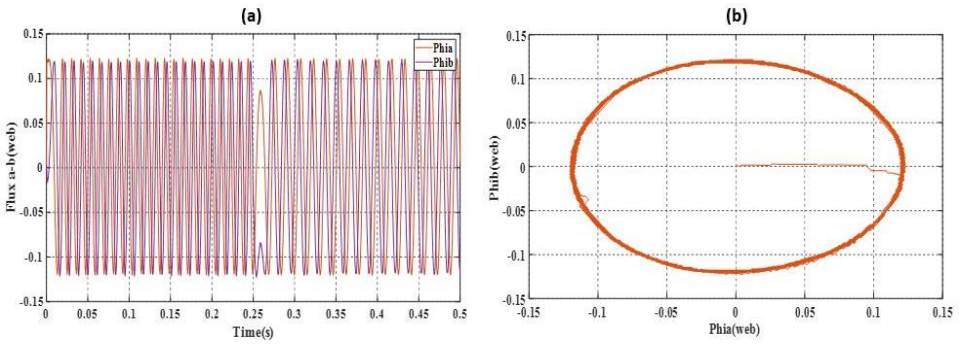

Fig. 10 (a) –The variation of stator flux (α, β) axes responses, (b) –The variation of stator flux (alpha) as a function of stator flux (beta).

5.2. Simulation Results of Predictive DTC-SVM

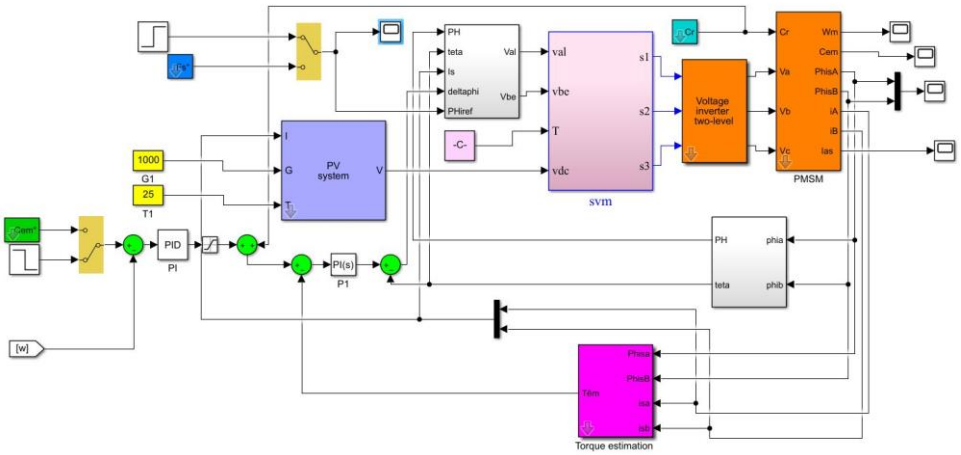

Fig. 11 The block diagram of the simulation of PMSM system control based on Predictive DTC-SVM

In the same operating condition (We apply a load of 5N.m at t = 0.3 and reverse direction of rotation at t = 0.2-0.25). In Fig.12.a, we note that the rotation speed makes a small overshoot at startup and then stabilizes at the rated speed 140 rad/s during a response time equal to 0.02 s. This overrun is justified by regulator values that have not been satisfactory and require adjustments. The electromagnetic torque, which is illustrated in Fig.12.b, perfectly follows its reference with an oscillation of 0.5N.m. On the curve of Fig.13.a, we see the stator current evolution which has a near sinusoidal shape with few fluctuations compared with the current of the DTC control. Concerning the Fig.13.b, we noticed that the modulus of the estimated stator flux revolves around its reference in a band of very narrow width that of the DTC. The presentation of the flow in the complex plane Fig.14.b shows that the stator flow starts from the point (0, 0) and then turns in the trigonometric direction to follow a circle of radius fixed by the instruction. Generally, we notice a decrease in torque and flux oscillations due to Predictive DTC-SVM control. Switching frequency in Predictive DTC-SVM is constant due to the excluded of the switching table and hysteresis regulators used in the conventional DTC and its replacement with PI controllers and SVM, which reduces the torque and flux oscillations as well as harmonic waves of constant current.

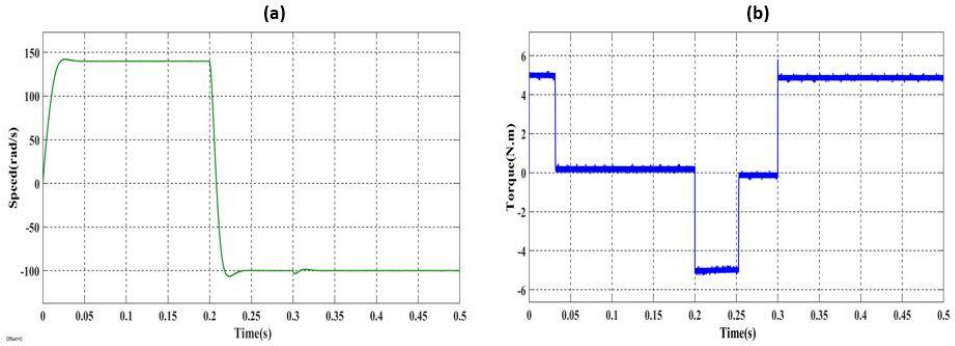

Fig. 11 (a) – The variation of speed responses, (b) –The variation of stator torque responses

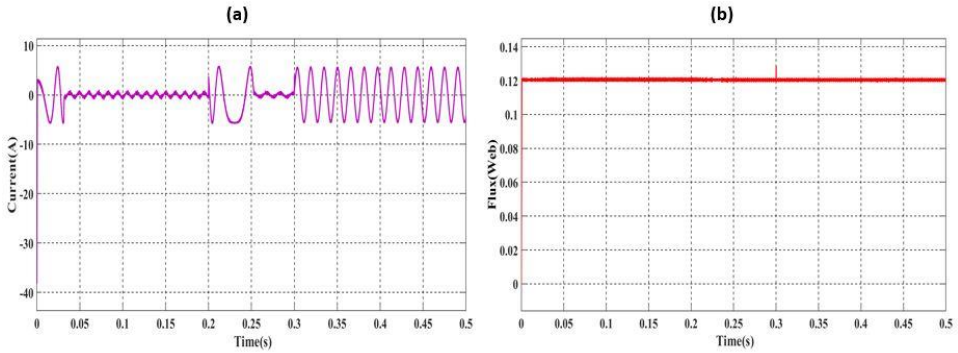

Fig. 12 (a) –The variation of current responses, (b) –The variation of flux responses

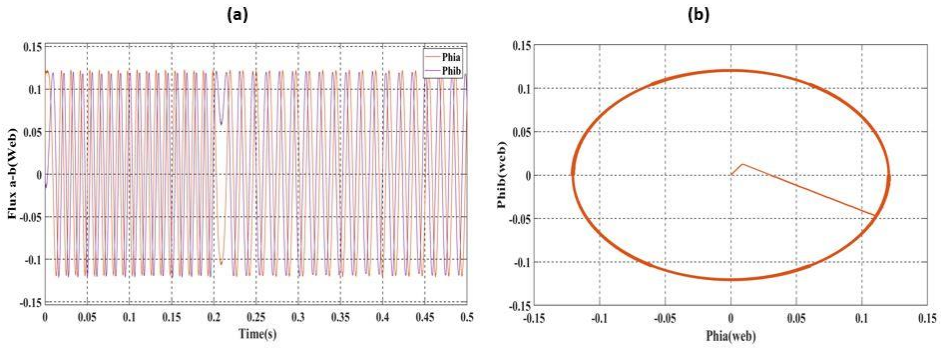

Fig. 13 (a) –The variation of stator flux (α, β) axes responses, (b) –The variation of stator flux (alpha) as a function of stator flux (beta).

The following table shows the difference between the conventional DTC and Predictive DTC-SVM:

Table 3 Various oscillations between the conventional DTC and Predictive DTC-SVM

oscillation	Torque (Nm)	Flux (wb)	Current (A)
DTC	2.5	0.01	4
DTC-SVM predictive	0.5	0.003	1.75

6. CONCLUSION

The work presented in this paper focuses on the study of Direct Torque Control (DTC) based on space vector modulation using predictive controller (Predictive SVM) of a permanent magnet synchronous motor (PMSM); indeed, this strategy is based on the direct determination of control sequence applied to the inverter. This control is less sensitive to the variation of the machine parameters and does not require mechanical sensors that are fragile. It has been concluded that the predictive SVM DTC control is to minimize ripple at the torque and flux, with a high switching frequency. From the results of the simulation can be summarized as follows:

- The oscillation of torque and flux is important in the conventional DTC because of the use of hysteresis regulators, which introduce limitations such as a high and uncontrollable switching frequency
- In DTC-SVM, we replace the hysteresis regulators and switching table with PI controller and SVM, the reducing of the oscillations in the torque and the flux produced by:
  - Inverter switching frequency is constant, which consequently reduces the flux stator and torque ripples as well as the harmonic waves of the stator current.
  - Distortion caused by sector changes are eliminated.
  - Zero low sampling frequency is required.
  - Dynamic performance of DTC-SVM are comparable with selection table based DTC.

In the end, the torque, flux and current was recorded 0.5, 0.003 and 1.75, respectively in DTC-SVM predictive and 2.5, 0.01 and 4 respectively in conventional DTC. The obtained results confirm that, the proposed control more applicable and compatible with our PMSM compared against the convectional DTC.

Acknowledgement: *This paper and the research behind it would not have been possible without the exceptional support of the General Directorate for Scientific Research and Technological Development, Algeria.*

REFERENCES

[1] O. Ellabban, H. Abu-Rub, F. Blaabjerg, "Renewable energy resources: Current status, future prospects and their enabling technology", *Renewable and Sustainable Energy Reviews*, vol. 39, pp. 748–764, 2014.

[2] A. Harrouz, A. Temmam, M. Abbes, "Renewable Energy in Algeria and Energy Management Systems", *International Journal of Smart Grid*, vol. 2, no. 1, 2018.

[3] A Harrouz, H Omar. Application of Solar Energies to Reinforce the Flow Water of Foggara in the Adrar Region. International Journal of Smart Grids, ijSmartGrid, 2(4), 203–208. (2018).

[4] A. Harrouz, M. Abbes, I. Colak, K. Kayisli, "Smart grid and renewable energy in Algeria", In Proceedings ogf the IEEE Xplore of Conference (ICRERA), 2017, San Diego, CA, USA.

[5] Y. Kim, H. T. Seo, S. K. Kim , K. S. Kim, "A robust current controller for uncertain permanent magnet synchronous motors with a performance recovery property for electric power steering applications", *Energies*, vol. 11, no. 5, p. 1224, 2018.

[6] Abd Essalam BADOUD, "MPPT Controller for PV Array under Partially Shaded Condition", *Algerian Journal of Renewable Energy and Sustainable Development*, vol. 01, no. 01, pp. 99–111, June 2019,

[7] Y. H. Kim, K. Choi, S. K. Kim, K. S. Kim, "A disturbance observer based approach to current control of PMSM drives for torque ripple reduction", *IFAC-Papers OnLine*, vol. 52, no. 4, pp. 206–209, 2009.

[8] A. V. Sant and K. R. Rajagopal, "PM Synchronous Motor Speed Control Using Hybrid Fuzzy-PI With Novel Switching Functions", *IEEE Transactions on Magnetics*, vol. 45, no. 10, October 2009.

[9] A. Ul Haq, D. Đurđanović, "Precedent-free fault localization and diagnosis for high speed train drive systems", *Facta Universitatis, Series Mechanical Engineering*, vol. 13, no. 2, pp. 67–79, 2015.

[10] M. Manohar, S Das, "Current sensor fault-tolerant control for direct torque control of induction motor drive using flux-linkage observer", *IEEE Transactions on Industrial Informatics*, vol. 13, no. 6, pp. 2824–2833, 2017.

[11] H. Mesloub, R. Boumaaraf, M. T. Benchouia, A. Golea, N. Goléa, K. Srairi, "Comparative study of conventional DTC and DTC SVM based control of PMSM motor - simulation and experimental results", In Proceedings of the International Association for Mathematics and Computers in Simulation (IMACS), 2018, vol. 18, pp. 30148-4.

[12] M. Lukac, M. Kameyama, M. Perkowski, P. Kerntopf, "Using homing, synchronizing and distinguishing input sequences for the analysis of reversible finite state machines", *Facta Universitatis, Series Electronics and Energetics*, vol. 32, no. 3, pp. 417–438, 2019.

[13] M. Amiri, J. Milimonfared, D. A. Khaburi, "Predictive torque control implementation for induction motors based on discrete space vector modulation", *IEEE Transactions on Industrial Electronics*, vol. 65, no. 9, pp. 6881–6889, 2018.

[14] F. Niu, X. Huang , L. Ge, J. Zhang, L. Wu, Y. Wang, K. Li , Y. Fang, "A Simple and Practical Duty Cycle Modulated Direct Torque Control for Permanent Magnet Synchronous Motors", *IEEE Transactions on Power Electronics*, vol. 34, no. 2, pp. 0885-8993, 2019.

[15] Dj. Rabah, B. Sid Ahmed, A. Samar, "Accurate computation of magnetic induction generated by hv overhead power lines", *Facta Universitatis, Series Electronics and Energetics*, vol. 32, no. 2, pp. 267–285, 2019.

[16] A. Ammar, A. Benakcha, A. Bourek, "Closed loop torque SVM-DTC based on robust super twisting speed controller for induction motor drive with efficiency optimization", *International Journal of Hydrogen Energy*, vol. 42, no. 28, pp. 17940–17952, 2017.

[17] M. Petronijevic, N. Mitrovic, V. Kostic, and B. Jovanovic, "Assessment of Unsymmetrical Voltage Sag Effectson AC Adjustable Speed Drives", *Facta Universitatis, Series: Electronics and Energetics*, vol. 22, no. 1, pp. 341–360, December 2009.

[18] A O. Conde, J. Francisco. G. Sánchez, J. Muci, A. S.González, "A review of diode and solar cell equivalent circuit model lumped parameter extraction procedures", *Facta Universitatis Series: Electronics and Energetics*, vol. 27, no. 1, pp. 57–102, March 2014.

[19] H. Bouzeriaa, C. Fethah, T. Bahib, I. Abadliab, Z. Layateb, S. Lekhchinec, "Fuzzy Logic Space Vector Direct Torque Control of PMSM for Photovoltaic Water Pumping System", *Energy Procedia*, vol. 74, pp. 760 – 771, 2015.

[20] S. Laribi, K. Mammar, F. Zohra Arama, T. Ghaitaoui, "Analyze of Impedance for Water Management in Proton Exchange Membrane Fue Fells Using Neural Networks Methodology", *Algerian Journal of Renewable Energy and Sustainable Development*, vol. 01, no. 01, pp. 96–105, June 2019,

[21] J. Francisco, S. García, R. Beatriz, "Modelling solar cell s-shaped i-v characteristics with dc lumped-parameter equivalent circuits - a review", *Facta Universitatis Series: Electronics and Energetics*, vol. 30, no. 3, pp. 327–350, September 2017.

[22] F. Zohra Arama, S. Laribi, T. Ghaitaoui, "A Control Method using Artificial Intelligence in Wind Energy Conversion System", *Algerian Journal of Renewable Energy and Sustainable Development*, vol. 01, no. 01, pp. 86–95, June 2019.

[23] A. Janjic, S. Savic, G. Janackovic, M. Stankovic, L. Zoran Velimirovic, "Multi-criteria assesment of the smart grid efficiency using the fuzzy analitical hyerarchy process", *Facta Universitatis, Series Electronics and Energetics*, vol. 29, no. 4, pp. 631–646, 2016.

[24] V. Kostić, M. Petronijević, N. Mitrović, B. Banković, "Experimental Verification of Direct Torque Control Methods for Electric Drive Applica", *Facta Universitatis, Series: Automatic Control and Robotics*, vol. 8, pp. 111–126, no. 1, 2009.

[25] A Sood, N Gupta, "Direct torque control scheme of induction motor drive using space vector Modulation", *International Journal of Recent Advances in Science and Technology*, vol. 6, no. 1, pp. 1–7, 2019.

[26] S. J. Kim, J. Park, D. H. Lee, "A Predictive DTC-PWM using 12 Vectors for Permanent Magnet Synchronous Motor", In 2019 10th International Conference on Power Electronics and ECCE Asia (ICPE 2019-ECCE Asia), 2019, pp. 2498–25.

[27] S. Krim, S. Gdaim, A. Mtibaa, And M.F. Mimouni, "FPGA Contribution in Photovoltaic Pumping Systems: Models of MPPT and DTC-SVM Algorithms", *International Journal of Renewable Energy Research*, vol. 6, no. 3, 2016.

[28] H. Abdelkader, F. Tahiri, B. Fatiha, B. Ibrahim, "Modelling and Simulation of Synchronous Inductor Machines", *Algerian Journal of Renewable Energy and Sustainable Development*, vol. 01, no. 01, pp. 8–23, June 2019.

[29] S. Krim, S. Gdaim, A. Mtibaa, M.F. Mimouni, "Hardware Implementation of a Predictive DTC-SVM with a Sliding Mode Observer of an Induction Motor on the FPGA", vol. 10, pp. 2224–2856, 2015.

[30] O. Ouledali, A. Meroufel, P. Wira, S. Bentouba, "Genetic Algorithm Tuned PI Controller on PMSM Direct Torque Control", *Algerian Journal of Renewable Energy and Sustainable Development*,vol. 1, no. 2, pp. 204–211, 2019.

[31] S. Belkacem, F. Naceri, R. Abdessemed, "A novel robust adaptive control algorithm and application to DTC-SVM of AC drives", *Serbian Journal of Electrical Engineering*, vol. 7, no. 1, pp. 21–40, 2010.

[32] M. Aleenejad, H. Mahmoudi, S. Jafarishiadeh, R. Ahmadi, "Fault-Tolerant Space Vector Modulation for Modular Multilevel Converters With Bypassed Faulty Submodules", *IEEE Transactions on Industrial Electronics*, vol. 66, no. 3, pp. 2463–2473, 2018.

[33] R. K. Pongiannan, S. Paramasivam, N. Yadaiah, "Dynamically Reconfigurable PWM Controller for Three-Phase Voltage-Source Inverters", *IEEE Transactions on power electronics*, vol. 26, no. 6, 2011.

[34] F. Tahiri, B. Fatiha, B. Ibrahim, O. Omar, H. Abdelkader, "Direct Torque Control (DTC) SVM Predictive of a PMSM Powered by a photovoltaic source", *Algerian Journal of Renewable Energy and Sustainable Development*, vol. 01, no. 01, pp. 1–7, June 2019.